

THE EVOLUTION OF THE $M_{\text{BH}}-\sigma$ RELATIONBRANT ROBERTSON^{1,4}, LARS HERNQUIST¹, THOMAS J. COX¹,
TIZIANA DI MATTEO², PHILIP F. HOPKINS¹, PAUL MARTINI¹, VOLKER SPRINGEL³*Draft version February 7, 2020*

ABSTRACT

We examine the evolution of the black hole mass - stellar velocity dispersion ($M_{\text{BH}}-\sigma$) relation over cosmic time using simulations of galaxy mergers that include feedback from supermassive black hole growth. Our calculations have been shown to reproduce the power-law scaling of the local, redshift zero $M_{\text{BH}}-\sigma$ relation and yield the observed normalization for an appropriate choice of the feedback efficiency. In the present paper, we consider mergers of galaxies varying the properties of the progenitors to match those expected at various cosmic times. In particular, we examine a range in redshifts $z = 0$ –6, where we modify the virial mass, gas fraction, interstellar medium equation of state, surface mass density, and concentration of the dark matter halos. We find that the slope of the resulting $M_{\text{BH}}-\sigma$ relation is the same at all redshifts. For the same feedback efficiency that reproduces the observed amplitude of the $M_{\text{BH}}-\sigma$ relation at $z = 0$, there is a weak redshift-dependence to the normalization, corresponding to an evolution in the Faber-Jackson relation, which results from an increasing velocity dispersion for a given galactic stellar mass. We develop a formalism to connect redshift evolution in the $M_{\text{BH}}-\sigma$ relation to the scatter in the local relation at $z = 0$. For an assumed model for the accumulation of black holes with different masses over cosmic time, we show that the scatter in the local relation places severe constraints on the redshift evolution of both the normalization and slope of the $M_{\text{BH}}-\sigma$ relation. Furthermore, we demonstrate that the cosmic downsizing of the black hole population introduces a black hole mass-dependent dispersion in the $M_{\text{BH}}-\sigma$ relation and that the skewness of the distribution about the locally observed $M_{\text{BH}}-\sigma$ relation is sensitive to redshift evolution in the normalization and slope. Improving the statistics of the local relation to measure the moments of its distribution will therefore make it possible to constrain the evolution of the $M_{\text{BH}}-\sigma$ relation and black hole population at redshifts that are currently not observationally accessible. In principle, these various diagnostics provide a method for differentiating between theories for producing the $M_{\text{BH}}-\sigma$ relation. In agreement with existing constraints, our simulations imply that hierarchical structure formation should produce the relation with small intrinsic scatter as the physical origin of the $M_{\text{BH}}-\sigma$ enjoys a remarkable resiliency to the redshift-dependent properties of merger progenitors.

Subject headings: galaxies: formation – galaxies: evolution

1. INTRODUCTION

Galactic spheroids exhibit a constitutive relation between their stellar kinematics and supermassive black holes (SMBHs) through observed correlations between black hole mass M_{BH} and either the bulge mass M_{bulge} (Miyoshi et al. 1995; Kormendy & Richstone 1995; Eckart & Genzel 1997; Faber et al. 1997; Magorrian et al. 1998; Ghez et al. 1998), or the velocity dispersion σ ($M_{\text{BH}}-\sigma$, Ferrarese & Merritt 2000; Gebhardt et al. 2000). The $M_{\text{BH}}-\sigma$ relation locally is a tight, power-law correlation with logarithmic slope originally estimated to be in the range $\beta \approx 3.75$ –4.8 (Ferrarese & Merritt 2000; Gebhardt et al. 2000). Later studies improved the accuracy of the local correlation (e.g. Tremaine et al. 2002, hereafter T02) and explored the relation between SMBH mass and other galaxy properties more fully (Wandel 2002; Ferrarese 2002; Marconi & Hunt 2003; Bernardi et al. 2003; Baes et al. 2003). Efforts to extend our knowledge of the connection between SMBHs and their host galaxies to higher redshifts include attempts to measure SMBH properties at $z = 4$ –6 (Vestergaard 2004) and to quantify the relation be-

tween SMBHs and galaxy kinematics in distant, active galaxies (Shields et al. 2003; Treu et al. 2004; Walter et al. 2004).

Observations of active galaxies at $z > 0$ have yielded ambiguous inferences about the nature of the $M_{\text{BH}}-\sigma$ at other redshifts, implying both redshift-dependent (Treu et al. 2004; Walter et al. 2004) and redshift-independent relations (Shields et al. 2003). Knowledge of the $M_{\text{BH}}-\sigma$ relation over cosmological time is crucial to understanding galaxy formation if SMBH feedback has a significant impact on this process (e.g. Springel et al. 2005; Robertson et al. 2005). The focus of our present work is to characterize the development of the $M_{\text{BH}}-\sigma$ relation over cosmic time with a large set of hydrodynamic simulations of galaxy mergers that include star formation and feedback from the growth of supermassive black holes, to use existing data to constrain redshift evolution in the $M_{\text{BH}}-\sigma$ relation, and to motivate specific observational tests for the $M_{\text{BH}}-\sigma$ relation at high redshifts using the next generation of large telescopes.

A variety of theoretical models have been proposed to explain the $M_{\text{BH}}-\sigma$ relation, based on physical mechanisms such as viscous disk accretion (Burkert & Silk 2001), adiabatic black hole growth (MacMillan & Henriksen 2002), gas or dark matter collapse (Adams et al. 2001; Balberg & Shapiro 2002; Adams et al. 2003), stellar capture by accretion disks (Miralda-Escudé & Kollmeier 2005), dissipationless merging (Ciotti & van Albada 2001; Nipoti et al. 2003), unregulated gas accretion (Archibald et al. 2002; Kazantzidis et al. 2005), and the self-regulated growth of black holes by momentum-

¹ Harvard-Smithsonian Center for Astrophysics, 60 Garden St., Cambridge, MA 02138, USA

² Carnegie-Mellon University, Department of Physics, 5000 Forbes Ave., Pittsburgh, PA 15213, USA

³ Max-Planck-Institut für Astrophysik, Karl-Schwarzschild-Straße 1, 85740 Garching bei München, Germany

⁴ brobertson@cfa.harvard.edu

TABLE 1.

Models	Progenitor V_{vir} [km s $^{-1}$]	Redshift z	Gas Fraction f_{gas}	ISM Pressurization q_{EOS}	Thermal Coupling η_{therm}
Local	80, 115, 160, 226, 320, 500	0	0.4, 0.8	0.25, 1.0	0.05
Intermediate- z	80, 115, 160, 226, 320, 500	2, 3	0.4, 0.8	0.25, 1.0	0.05
High- z	115, 160, 226, 320, 500	6	0.4, 0.8	0.25, 1.0	0.05
Low η_{therm}	115, 160, 226, 320, 500	6	0.4, 0.8	0.25, 1.0	0.025

or pressure-driven winds (Silk & Rees 1998; King 2003; Murray et al. 2005; Di Matteo et al. 2005; Sazonov et al. 2005). An important outcome of these studies has been the recognition that the growth of SMBHs may have important consequences cosmologically, especially for galaxy formation, motivating work linking the hierarchical growth of structure with the evolution or demographics of SMBHs through studies of quasar evolution (Haiman & Loeb 1998; Richstone et al. 1998; Fabian 1999; Monaco et al. 2000; Kauffmann & Haehnelt 2000; Haehnelt & Kauffmann 2000; Granato et al. 2001; Menou et al. 2001; Menci et al. 2003; Di Matteo et al. 2003, 2004; Wyithe & Loeb 2003; Wyithe 2005; Hopkins et al. 2005a,b,c,d) and the formation of normal galaxies (Volonteri et al. 2003; Cox et al. 2005; Robertson et al. 2005).

Motivated by the long-standing view that mergers form spheroids (e.g. Toomre 1977), Di Matteo et al. (2005) studied the self-regulated growth of black holes in galaxy collisions and showed that this process can reproduce the $M_{\text{BH}}-\sigma$ relation at $z=0$ for progenitors similar to local galaxies. In this paper we use the Di Matteo et al. (2005) model to explicitly calculate the behavior of the $M_{\text{BH}}-\sigma$ relation with cosmic time induced by the redshift-scalings of galaxy properties. Using a large set of hydrodynamical simulations of mergers that include feedback from supernovae and accreting SMBHs, the resulting $M_{\text{BH}}-\sigma$ relation is calculated for galaxy models that span a large range in virial mass, gas fraction, interstellar medium equation of state, surface mass density, dark matter concentration, and redshift.

We determine the allowed redshift evolution in either the normalization or slope of the $M_{\text{BH}}-\sigma$ relation consistent with constraints from the observed $M_{\text{BH}}-\sigma$ relation at $z=0$ under the assumption that black holes of mass M_{BH} form at a characteristic epoch z_f . The redshift evolution of the normalization in our simulations yields a dispersion in the $z=0$ relation consistent with the observed scatter. We further relate our simulations to ongoing efforts to measure the $M_{\text{BH}}-\sigma$ relation in high-redshift active galactic nuclei (AGN), and discuss future observational tests for normal galaxies at high redshifts with the next-generation of large aperture telescopes.

We describe our simulation methodology in §2, report our results in §3, compare with observational constraints in §4, discuss our results in §5, and summarize and conclude in §6. For our cosmological parameters, we adopt a flat universe with $\Omega_m = 0.3$, $\Omega_\Lambda = 0.7$, $\Omega_b = 0.04$, and $h = 0.7$.

2. METHODOLOGY

We have performed a set of 112 simulations of merging galaxies using the entropy-conserving formulation (Springel & Hernquist 2002) of smoothed particle hydrodynamics (Lucy 1977; Gingold & Monaghan 1977) as implemented in the GADGET code (Springel et al. 2001; Springel 2005). Each progenitor galaxy is constructed using the method described by Springel et al. (2004), generalized to al-

low for the expected redshift scaling of galaxy properties. For a progenitor with virial velocity V_{vir} at redshift z we determine a virial mass and radius assuming a virial overdensity $\Delta_{\text{vir}} = 200$ times the critical density, using the relations

$$M_{\text{vir}} = \frac{V_{\text{vir}}^3}{10GH(z)} \quad (1)$$

$$R_{\text{vir}} = \frac{V_{\text{vir}}}{10H(z)}. \quad (2)$$

For the Navarro-Frenk-White concentration (Navarro et al. 1997) of each progenitor dark matter halo, we follow Bullock et al. (2001) and adopt

$$C_{\text{vir}} \simeq 9 \left[\frac{M_{\text{vir}}}{M_{\star}(z=0)} \right]^{-0.13} (1+z)^{-1} \quad (3)$$

where $M_{\star}(z=0) \sim 8 \times 10^{12} h^{-1} M_{\odot}$ is the linear collapse mass at the present epoch and $H(z)$ is the Hubble parameter. The concentration and virial radius are then used to create Hernquist (1990) profile dark matter halos using the conversion described by Springel et al. (2004). The halos are populated with exponential disks of mass $M_{\text{disk}} = 0.041 M_{\text{vir}}$ and fractional gas content f_{gas} , whose scalelengths R_d are determined using the Mo et al. (1998) formalism assuming the specific angular momentum content j_d equals the disk mass fraction m_d and a constant halo spin $\lambda = 0.033$. The distribution of halo spins in dissipationless simulations is measured to be independent of mass and redshift (Vitvitska et al. 2002) and our chosen value for λ is near the mode of the distribution. The vertical scale heights of the stellar disks are set to $0.2R_d$, similar to the Milky Way scaling (Siegel et al. 2002). The vertical scale heights of the gaseous disks are determined via an integral constraint on the surface mass density, a self-consistent determination of the galaxy potential, and the effective equation of state (EOS) of the multiphase interstellar medium (ISM, McKee & Ostriker 1977; Springel & Hernquist 2003). The pressurization of the ISM can be varied using an equation of state softening parameter q_{EOS} (for details, see Springel et al. 2004), which linearly interpolates between isothermal gas ($q_{\text{EOS}} = 0$) and a strongly pressurized multiphase ISM ($q_{\text{EOS}} = 1$).

Each initial galaxy model consists of 40,000 gas particles, 60,000 dark matter particles, and 40,000 stellar particles. The gravitational softening of gas and stellar particles is set to $100h^{-1}(1+z)^{-1}$ pc. The progenitors merge on prograde-parabolic orbits, with an initial separation $R_{\text{init}} = 5R_{\text{vir}}/8$ and pericentric distance $R_{\text{peri}} = 2R_d$. Each progenitor galaxy contains a “sink” particle with a black hole seed of mass $10^5 h^{-1} M_{\odot}$ allowed to grow through a model based on Bondi-Hoyle-Lyttleton accretion (Hoyle & Lyttleton 1939; Bondi & Hoyle 1944; Bondi 1952). In this model, a fraction $\epsilon_r = 0.1$ of the mass accretion rate $\dot{M}c^2$ is radiated and a fraction $\eta_{\text{therm}} = 0.05$ of this 10% is deposited as thermal feedback into the surrounding gas. The thermal coupling is cali-

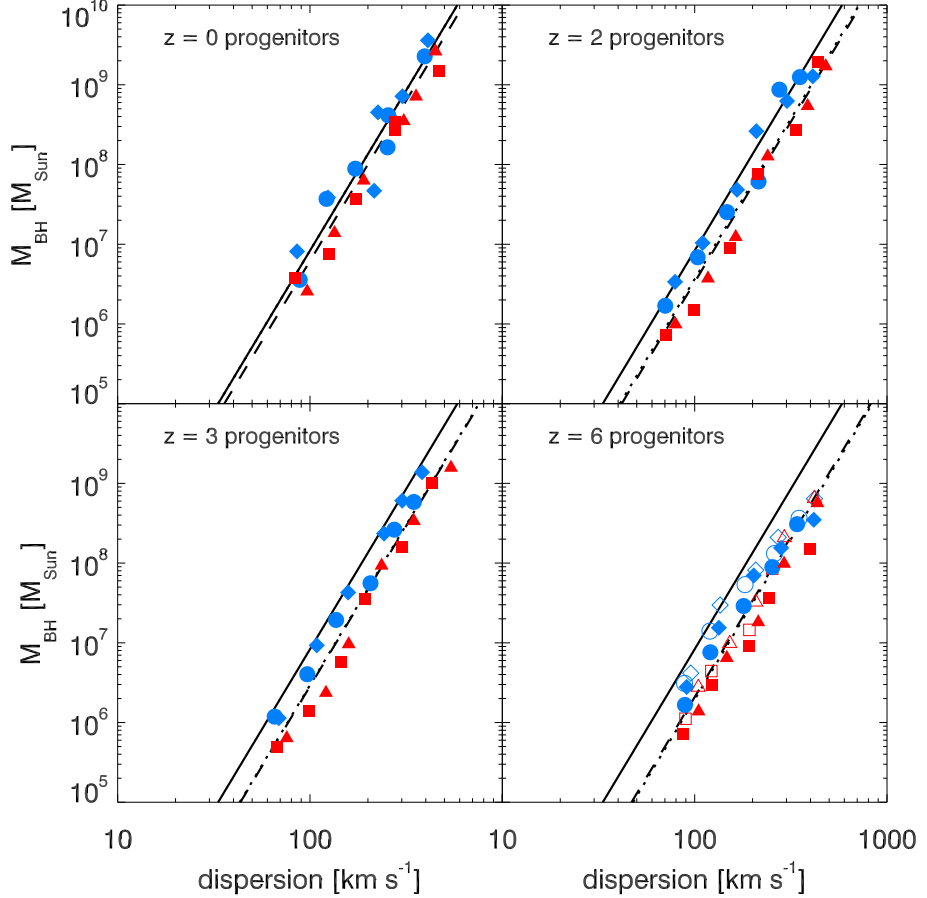


FIG. 1.— Relation between black hole mass M_{BH} and stellar velocity dispersion σ for redshift $z = 0, 2, 3$, and 6 progenitors. At each redshift we vary the gas fraction f_g and the pressurization of the interstellar medium q_{EOS} (see Springel et al. 2005), and we plot results for M_{BH} and σ in progenitor models with $g_f = 0.4, q_{\text{EOS}} = 0.25$ (blue circles), $g_f = 0.8, q_{\text{EOS}} = 0.25$ (blue diamonds), $g_f = 0.4, q_{\text{EOS}} = 1.0$ (red squares), and $g_f = 0.8, q_{\text{EOS}} = 1.0$ (red triangles). The Tremaine et al. (2002) best fit to the local $M_{\text{BH}} - \sigma$ relation (black line) is plotted for reference. The simulated $M_{\text{BH}} - \sigma$ relations display a weak redshift evolution in their normalization of the form $\sigma \sim \sigma_{z=0} (1+z)^\xi$, and we plot the best fit evolution assuming either the observed normalization at $z=0$ ($\xi = 0.186$, dotted lines) or the best fit $z=0$ normalization measured from the simulations ($\xi = 0.138$, dashed lines). Also shown is the $M_{\text{BH}} - \sigma$ relation for $z=6$ progenitors calculated assuming a decreased thermal coupling for black hole feedback (open symbols). Lowering the thermal coupling for black hole feedback by half results in only a small increase in the final black hole mass.

brated to reproduce the normalization of the local $M_{\text{BH}} - \sigma$ relation (Di Matteo et al. 2005). As our intent is to calculate the development of the $M_{\text{BH}} - \sigma$ relation over time and to avoid assumptions about the presence or form of the $M_{\text{BH}} - \sigma$ relation at higher redshifts, the progenitor models do not contain bulges but instead yield an $M_{\text{BH}} - \sigma$ relation self-consistently through the merger process.

We simulate equal-mass mergers of progenitors appropriate for redshifts $z = 0, 2, 3$, and 6 with virial velocities in the range $V_{\text{vir}} = 80 - 500 \text{ km s}^{-1}$. For each virial velocity, progenitors with gas fractions $f_{\text{gas}} = 0.4, 0.8$ and EOS softenings $q_{\text{EOS}} = 0.25, 1.0$ are simulated. The $z = 6$ runs are also repeated using a thermal coupling constant of $\eta_{\text{therm}} = 0.025$ to gauge the effect of altering the efficiency with which black hole feedback heats the surrounding ISM. Table 1 summarizes our full set of simulations.

After the completion of a merger, the projected half-mass effective radius R_e and the mass-weighted line-of-sight stellar velocity dispersion σ measured within an aperture of radius R_e is calculated for each remnant galaxy for many viewing angles. This determination of σ for simulated systems is commensurate with the observational method of Gebhardt et al.

(2000) that measures a luminosity-weighted velocity dispersion within an effective radius. The black hole mass M_{BH} in each galaxy is tracked during the simulation and compared with the average dispersion σ to examine any resulting $M_{\text{BH}} - \sigma$ correlation.

3. RESULTS

Figure 1 shows the $M_{\text{BH}} - \sigma$ relation produced by the merging of progenitor galaxies appropriate for redshifts $z = 0, 2, 3$, and 6 (upper left to bottom right). At each redshift, we perform a least-squares fit to the $M_{\text{BH}} - \sigma$ relation of the form

$$\log M_{\text{BH}} = \alpha + \beta \log(\sigma/\sigma_0) \quad (4)$$

where the relation is defined relative to $\sigma_0 = 200 \text{ km s}^{-1}$. The observed relation has a normalization coefficient $\alpha = 8.13$ and slope $\beta = 4.02$ (T02, solid line). Table 2 lists the best fit α and β from the simulations at each redshift, along with the dispersion $\Delta_{\log M_{\text{BH}}}$ about each best fit relation. Table 2 also reports the best fit normalization $\alpha^{\beta=4.02}$ and resultant dispersion $\Delta_{\log M_{\text{BH}}}^{\beta=4.02}$ assuming the slope of the $M_{\text{BH}} - \sigma$ relation is a constant $\beta = 4.02$ with redshift. The intrinsic $M_{\text{BH}} - \sigma$ dispersion at any given redshift induced by varying the gas fraction

TABLE 2. BEST FIT $M_{\text{BH}}-\sigma$ RELATIONS

Progenitor Redshift	α	β	$\Delta_{\log M_{\text{BH}}}$	$\alpha^{\beta=4.02}$	$\Delta_{\log M_{\text{BH}}}^{\beta=4.02}$
$z=0$	8.01	3.87	0.26	8.01	0.26
$z=2$	7.83	4.10	0.28	7.83	0.28
$z=3$	7.72	4.02	0.26	7.72	0.26
$z=6$	7.44	3.62	0.24	7.45	0.26

or ISM equation of state is similar to the observed dispersion $\Delta_{\log M_{\text{BH}}} = 0.25 - 0.3$ (T02). As Figure 1 and Table 2 demonstrate, an $M_{\text{BH}}-\sigma$ relation consistent with a power-law scaling of index $\beta \simeq 4$ is predicted by our modeling for normal galaxies out to high redshift. We infer that the physics that sets the scaling of the $M_{\text{BH}}-\sigma$ relation is insensitive to an extremely wide range of galaxy properties. Virial velocities of the progenitors range from $V_{\text{vir}} = 80 \text{ km s}^{-1}$ to $V_{\text{vir}} = 500 \text{ km s}^{-1}$ at each redshift while the dark matter concentrations range from $C_{\text{vir}} \simeq 15.6$ in the smallest progenitor at $z=0$ to $C_{\text{vir}} \simeq 1.5$ in the largest progenitor at $z=6$. For the $M_{\text{BH}}-\sigma$ relation at each redshift, models with moderate ISM pressurization typically experience slightly more black hole growth than models with strong ISM pressurization. The increased thermal feedback in the model with a stiffer equation of state improves the dynamical stability of the gas, lessens gas angular momentum loss during the merger (Robertson et al. 2004, 2005), and results in less fueling of the black hole (Hopkins et al. 2005e).

3.1. The Normalization of the $M_{\text{BH}}-\sigma$ Relation with Redshift

The normalization of the $M_{\text{BH}}-\sigma$ relation evolves weakly with redshift relative to the observed $z=0$ result. To characterize this, we generalize the parameterization of the $M_{\text{BH}}-\sigma$ relation to the form

$$\log M_{\text{BH}} = \alpha + \beta \log(\sigma/\sigma_0) - \xi \log(1+z) \quad (5)$$

with ξ defined to be positive if the characteristic black hole mass decreases with redshift or the characteristic velocity dispersion increases with redshift. We determine the value of ξ for our simulations assuming either the observed $z=0$ normalization $\alpha_{\text{obs}} = 8.13$ (Figure 1, dotted line) or the calculated $z=0$ normalization $\alpha_{\text{calc}} = 8.01$ (Figure 1, dashed line) with the slope fixed at $\beta = 4.02$. We find evidence for a weak evolution, with $\xi = 0.186$ for α_{obs} and $\xi = 0.138$ for α_{calc} using the best-fit parameters reported in Table 2. We now consider whether the weak evolution we find in the normalization of the $M_{\text{BH}}-\sigma$ relation represents a physical effect caused by the redshift-dependent properties of the progenitors or is an artifact of our modeling.

3.1.1. Systematic Considerations

The systematic effects of our modeling include the redshift-scaling of halo virial properties and an assumed fixed thermal coupling of black hole feedback to the gas in our simulations. The form of the progenitor galaxies is inferred from the linear theory of dissipational galaxy formation and is therefore idealized, but in the absence of cosmological simulations with comparable resolution that include feedback from SMBH growth, our choice appears well-motivated. While the model considered here assumes a fixed thermal coupling for black hole feedback, if the thermal coupling changes with some bulk property of galaxies with redshift (metallicity, for example) then this assumption may influence our results. The

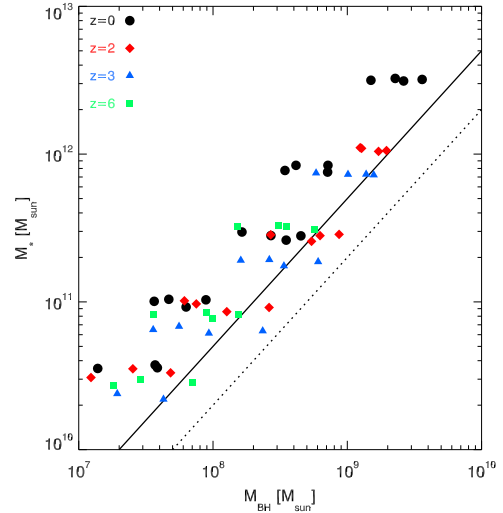


FIG. 2.— Relation between total stellar mass M_{\star} and black hole mass M_{BH} for merger progenitors appropriate for redshifts $z=0$ (black circles), $z=2$ (red diamonds), $z=3$ (blue triangles), and $z=6$ (green squares). At each circular velocity and redshift, four models for the gas fraction and interstellar medium equation of state are considered. We plot bulge-dominated remnants only. The $M_{\text{BH}}-M_{\text{bulge}}$ relations observed by Marconi & Hunt (2003) (solid line) and Magorrian et al. (1998) (dotted line) are shown for comparison. The ratio of black hole to stellar mass remains roughly constant for progenitors of all redshifts we consider.

magnitude of thermal coupling $\eta_{\text{therm}} = 0.05$ of black hole feedback to the surrounding gas is calibrated to reproduce the locally observed relation. To illustrate the impact of this choice, Figure 1 shows the change in normalization of the $M_{\text{BH}}-\sigma$ relation for $z=6$ progenitors introduced by lowering the thermal coupling parameter to $\eta_{\text{therm}} = 0.025$ (open symbols, lower right panel). As the coupling of the feedback to the gas of the galaxy is decreased, the rate of energy input to the surrounding material by a black hole of a given mass and accretion rate is lessened. The transition between Eddington-limited and self-regulated growth then occurs at a correspondingly higher black hole mass and, as a result, the final mass of the SMBH increases. Decreasing the thermal coupling also mildly flattens the slope of the relation for the highest mass black holes. Overall, the change in the thermal coupling does not re-normalize the $M_{\text{BH}}-\sigma$ relation for $z=6$ progenitors to coincide with the T02 result. We also note that varying the gas fraction in the progenitors from $f_{\text{gas}} = 0.4$ to $f_{\text{gas}} = 0.8$ has little effect on either the normalization or the scaling of the relation at any given redshift.

A sensible measure to gauge a possible evolution of the black hole growth with redshift is the comparison of black hole mass M_{BH} with total stellar mass M_{\star} , which serves as a convenient proxy for the observed $M_{\text{BH}}-M_{\text{bulge}}$ relation. Figure 2 shows the $M_{\text{BH}}-M_{\star}$ relation for mergers at all redshifts we consider, with the Marconi & Hunt (2003) (solid line) and Magorrian et al. (1998) (dotted line) $M_{\text{BH}}-M_{\text{bulge}}$ relations plotted for comparison. We show the largest stellar mass systems, which are mostly spheroidal and lie near the Marconi & Hunt (2003) relation. Any redshift-dependent impact on the black hole mass at a given stellar mass is not discernibly stronger than the black hole mass increase for decreasing ISM pressurization and increasing gas fraction. We therefore conclude that the systematic uncertainties of our modeling do not generate an unphysical evolution in the black

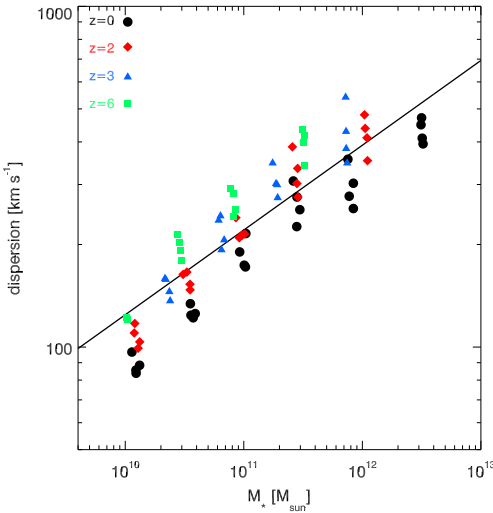


FIG. 3.— Relation between stellar velocity dispersion σ and total stellar mass M_* of remnants for merger progenitors appropriate for redshifts $z = 0$ (black circles), $z = 2$ (red diamonds), $z = 3$ (blue triangles), and $z = 6$ (green squares). At each circular velocity and redshift, four models for the gas fraction and interstellar medium equation of state are considered. A total stellar mass version of the Faber & Jackson (1976) relation constructed by combining the Tremaine et al. (2002) $M_{\text{BH}}-\sigma$ and Marconi & Hunt (2003) $M_{\text{BH}}-M_{\text{bulge}}$ relations is shown for comparison (solid line). The increasing velocity dispersion for a given stellar mass with redshift, which can be viewed as a weak evolution in the Faber-Jackson relation, is responsible for the corresponding evolution in the calculated $M_{\text{BH}}-\sigma$ relation.

hole mass. Instead, it appears more likely that the variation of the normalization of the $M_{\text{BH}}-\sigma$ relation with redshift has a physical origin in the structural changes of the merging galaxies, a possibility we examine next.

3.1.2. Physical Considerations

The redshift-dependent structure of progenitor systems expected from the cosmological scalings of galaxy properties provides a plausible explanation for the weak evolution in the normalization of the $M_{\text{BH}}-\sigma$ relation with redshift. For example, the depth of the potential well in the center of each remnant will influence the velocity dispersion, while for the regions where the baryons dominate the stellar mass of the spheroid determines the potential. The characteristic densities of the progenitors and remnants increase with redshift and any relation involving the stellar mass may evolve cosmologically. Similar trends can be measured with our simulations. Figure 3 shows the stellar velocity dispersion as a function of the total stellar mass of each remnant for the simulations at each redshift, along with a stellar mass formulation of the Faber-Jackson luminosity-stellar velocity dispersion relation found from the combination of the Marconi & Hunt (2003) $M_{\text{BH}}-M_{\text{bulge}}$ and T02 $M_{\text{BH}}-\sigma$ relations (solid line). For a given stellar mass, the velocity dispersion increases for higher redshift progenitors, with the greatest increase for the most spheroid-dominated systems. We therefore ascribe the weak evolution in the normalization of the $M_{\text{BH}}-\sigma$ relation with redshift to a systematically increasing σ for a given M_{BH} or M_* , and argue that the steeper potential wells of high redshift galaxies is a primary cause for this apparent redshift evolution in the stellar mass formulation of the Faber-Jackson relation.

The evolution of the stellar velocity dispersion for a given stellar mass between redshifts $z = 2$ and $z = 6$ can be com-

pared with the redshift-dependent properties of our progenitor models. Changes in the structure of galaxies can lead to an evolution in the stellar velocity dispersion that scales with redshift in a similar fashion to the evolving normalization in our calculated $M_{\text{BH}}-\sigma$ relations at redshifts $z = 2-6$. A possible origin for these effects can be illustrated by the use of a simple galaxy model that demonstrates the impact of redshift-dependent structural properties on the central stellar kinematics. To demonstrate this, we consider the velocity dispersion of a stellar spheroid residing within a dark matter halo with fixed virial mass M_{vir} as a function of redshift. For simplicity, we assume that the stellar mass within the halo is a fixed fraction of the virial mass and that the central potential is dominated by the baryons. We model both the dark matter halo and stellar spheroid as Hernquist profiles with the stellar spheroid scalelength a_s a fraction b of the halo scalelength a_h . Equations (1–3) describe the redshift scalings of the dark matter halos for a given virial velocity V_{vir} . Incorporating the results from Springel et al. (2004), we find the spheroid scalelength will depend on virial mass and redshift as

$$a_s(M_{\text{vir}}, z) = \frac{b}{C_{\text{vir}}} \sqrt{2 \left[\ln(1 + C_{\text{vir}}) - C_{\text{vir}}/(1 + C_{\text{vir}}) \right]} \quad (6)$$

$$\times [GM_{\text{vir}}]^{1/3} [10H(z)]^{-2/3}$$

where C_{vir} is the mass- and redshift-dependent concentration given by Equation (3). The stellar velocity dispersion of the Hernquist profile depends on the scalelength as $\sigma \propto a_s^{-1/2}$. The power-law scaling of $\sigma \propto (1+z)^\xi$ for $2 < z < 6$ then ranges from $\xi \approx 0.17$ for a $M_{\text{vir}} \sim 10^{10} M_\odot$ halo to $\xi \approx 0.28$ for $M_{\text{vir}} \sim 10^{14} M_\odot$, which encompasses the approximate scaling ξ found in the simulations. Below redshift $z = 2$, the redshift evolution of the stellar velocity dispersion begins to flatten and is roughly constant between redshifts $z = 0$ and $z = 1$. The relative constancy of the stellar velocity dispersion in this redshift regime is caused by the growing influence of the cosmological constant on the Hubble parameter as it balances the increase in the virial concentration. We therefore expect the normalization of the $M_{\text{BH}}-\sigma$ relation to remain roughly fixed for purely dissipationless systems between $z = 0$ and $z = 1$, and begin to evolve roughly as a weak power-law in $1+z$ toward higher redshifts. For the dissipational systems we simulate, an additional increase in the stellar velocity dispersion between redshifts $z = 0$ and $z = 2$ beyond the estimate for purely stellar systems is needed to fully explain the evolution measured in the simulations by redshift $z = 2$. We leave such an exploration for future work, but note here that either gas dissipation or feedback effects from the supermassive black hole may influence the scaling of the stellar dispersion with redshift or its mass dependence.

4. COMPARISON WITH OBSERVATIONS

4.1. Scatter Induced in the Local $M_{\text{BH}}-\sigma$ Relation by Redshift Evolution

If the $M_{\text{BH}}-\sigma$ relation evolves with redshift, any redshift evolution in the cosmic black hole population will affect the statistical distribution of galaxies about the observed $M_{\text{BH}}-\sigma$ relation at $z = 0$. Following the formalism presented by Yu & Lu (2004, YL04), we can statistically characterize the connection between active galactic nuclei and the local $M_{\text{BH}}-\sigma$ relation by assuming BH growth occurs primarily during periods of quasar activity. If we further assume that the $M_{\text{BH}}-\sigma$ relation generated by mergers at each redshift has

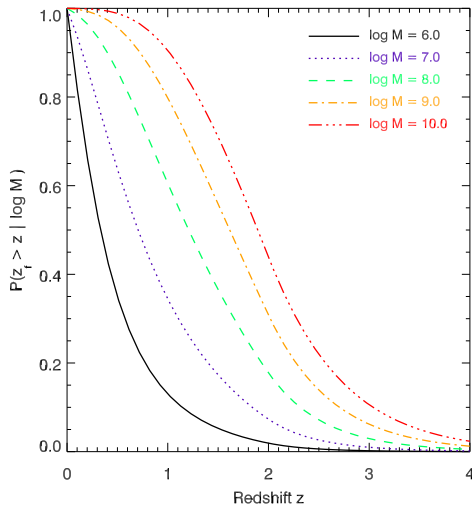


FIG. 4.— Integrated probability distribution function $P(z_f > z | \log M_{\text{BH}})$ for a supermassive black hole of mass M_{BH} to have formed at a redshift $z_f > z$, as determined by the best fit model of Hopkins et al. (2005e) (see §4.1 for details). Shown is the $P(z_f > z | \log M_{\text{BH}})$ for $\log M_{\text{BH}} = 6.0$ (solid black), 7.0 (purple dotted), 8.0 (blue dashed), 9.0 (green dash-dotted), and 10.0 (red dash-double dotted). More massive black holes are primarily formed at successively higher redshifts, reflecting the cosmic downsizing trend inferred from evolution in the quasar luminosity function.

an intrinsically small scatter, we can calculate the allowed redshift evolution in σ given M_{BH} consistent with the dispersion measured in the local $M_{\text{BH}}-\sigma$ relation.

From $P(z_f | \log M_{\text{BH}})$, the probability distribution function (PDF) for a black hole of mass M_{BH} to have formed at a redshift z_f , we can calculate the expectation value of a function $q(z_f, \log M_{\text{BH}})$ given $\log M_{\text{BH}}$ as

$$\langle q | \log M_{\text{BH}} \rangle = \int q(z_f, \log M_{\text{BH}}) P(z_f | \log M_{\text{BH}}) dz_f \quad (7)$$

and the moments about $\langle q | \log M_{\text{BH}} \rangle$ as

$$\begin{aligned} \mu_n^q = & \int [q(z_f, \log M_{\text{BH}}) - \langle q | \log M_{\text{BH}} \rangle]^n \\ & \times P(z_f | \log M_{\text{BH}}) dz_f. \end{aligned} \quad (8)$$

We can identify the expectation value $\langle \sigma | \log M_{\text{BH}} \rangle$ with the $M_{\text{BH}}-\sigma$ relation observed at $z = 0$, and associate the second moment with the measured $M_{\text{BH}}-\sigma$ relation dispersion $\Delta_{\log M_{\text{BH}}}^{\text{obs}} \equiv \sqrt{\mu_2^{\sigma}} = 0.25 - 0.3$ dex (T02). If the velocity dispersion depends on some larger set of independent variables \bar{x} as $\sigma(\log M_{\text{BH}}, \bar{x})$, and $P(z_f | \log M_{\text{BH}})$ is independent of \bar{x} , we can extend this definition of the expectation value to calculate, e.g., $\langle \sigma | \log M_{\text{BH}}, \bar{x} \rangle$. The analysis of YL04 treats a more general scenario where joint PDFs for properties associated with black hole mass are functions of more than one variable, and we restrict our attention to a single PDF directly relating z_f and $\log M_{\text{BH}}$. Equivalently, that $P(z_f | \log M_{\text{BH}})$ is independent of \bar{x} reflects our operating assumptions including: 1) all scatter in the $M_{\text{BH}}-\sigma$ at $z = 0$ owes to evolution in σ with redshift (i.e. if \bar{x} is null, σ does not depend on z and the dispersion in the $M_{\text{BH}}-\sigma$ relation would be $\Delta_{\log M_{\text{BH}}} = 0$) and 2) galactic evolution subsequent to the primary growth phase of the black hole does not affect the direct connection between z_f and $\log M_{\text{BH}}$.

The $M_{\text{BH}}-\sigma$ relation generated by the merging of progenitor galaxies appropriate for a range of redshifts demonstrates an evolution in its normalization with respect to the observed relation at $z = 0$. By utilizing a known $P(z_f | \log M_{\text{BH}})$ and a functional form for $\sigma(z, \log M_{\text{BH}}, \bar{x})$ that captures this evolution, the dispersion about the average relation $\langle \sigma | \log M_{\text{BH}}, \bar{x} \rangle$ can be calculated and compared with the observed $\Delta_{\log M_{\text{BH}}}^{\text{obs}}$. The small observed scatter in the $M_{\text{BH}}-\sigma$ relation will then constrain \bar{x} for a known $P(z_f | \log M_{\text{BH}})$. To this end, we consider $M_{\text{BH}}-\sigma$ relations with an evolution in normalization of the form of Equation (5) with the identification of $\bar{x} = \xi$, or an evolution in the slope of the form

$$\log M_{\text{BH}} = \alpha + \beta(1+z)^{\phi} \log(\sigma/\sigma_0) \quad (9)$$

with $\bar{x} = \phi$. We proceed to calculate the resulting variance μ_2^{σ} about the mean $M_{\text{BH}}-\sigma$ relation at $z = 0$, using these forms for $\sigma(M_{\text{BH}}, z)$ and the observed values of $\alpha = 4.0$, $\beta = 8.13$ (T02). As the sign of either ϕ or ξ will strongly affect the symmetry of the inferred distribution about the mean relation, we also characterize the skewness $\gamma_1 = \mu_3^{\sigma}/(\mu_2^{\sigma})^{3/2}$.

We now adopt a form for $P(z_f | \log M_{\text{BH}})$, using the results of Hopkins et al. (2005e, H05), and calculate the probability $P(z_f | \log M_{\text{BH}})$ for a black hole of mass M_{BH} to have formed at redshift z_f . The H05 modeling uses luminosity-dependent quasar lifetimes and obscuring column density distributions measured from the simulations presented in this paper to infer the black hole mass function $n(M_{\text{BH}}, z)$ from a host of constraints from observations of quasars. The evolution of $n(M_{\text{BH}}, z)$ with redshift is primarily determined by an evolving characteristic luminosity $L_{\star}(z)$ that determines the location of the maximum of $n(M_{\text{BH}}(L), z)$. In principle, $P(z_f | \log M_{\text{BH}})$ is well determined in the context of the H05 model for the cosmic black hole population via the observed evolution of quasar luminosity functions in multiple wavebands and constraints on the mass density of black holes at $z = 0$. In practice, the somewhat weak observational constraint on the evolution of the break in the luminosity function at the highest observationally-accessible redshifts requires a choice for the functional form of the evolving characteristic luminosity $L_{\star}(z)$ that determines the peak of the black hole mass function $n(M_{\text{BH}}(L), z)$. As an *Ansatz* we adopt the form for $L_{\star}(z)$ chosen by H05 to best fit the available constraints from observations, though we note that the calculations presented in section §6 of H05 and below can be applied to more general forms of $n(M_{\text{BH}}, z)$ and $L_{\star}(z)$ and the analysis presented here could be repeated for other interpretations of the quasar luminosity function than that adopted by H05.

The resulting $P(z_f | \log M_{\text{BH}})$, plotted in an integral form in Figure 4 and reproduced from H05, reflects the best fit model for the evolution of the cosmic black hole population given the available data and the H05 interpretation of the quasar luminosity function. Cosmic downsizing, the concept that black holes of larger mass formed characteristically at higher redshifts (e.g. Cowie et al. 2003; Steffen et al. 2003), is apparent in our $P(z_f | \log M_{\text{BH}})$ as the formation-redshift PDF for low mass black holes increases strongly at low redshifts. The characteristic downsizing of black hole masses as the universe ages leads to an immediate general conclusion about possible evolution in the $M_{\text{BH}}-\sigma$ relation: if black holes of differing masses form at different characteristic redshifts, any evolution in the $M_{\text{BH}}-\sigma$ relation will introduce an M_{BH} -dependent dispersion in the observed relation at $z = 0$. While subsequent processes may reduce or amplify the mass dependence of $\Delta_{\log M_{\text{BH}}}$, if observations reveal a trend in $\Delta_{\log M_{\text{BH}}}$ between

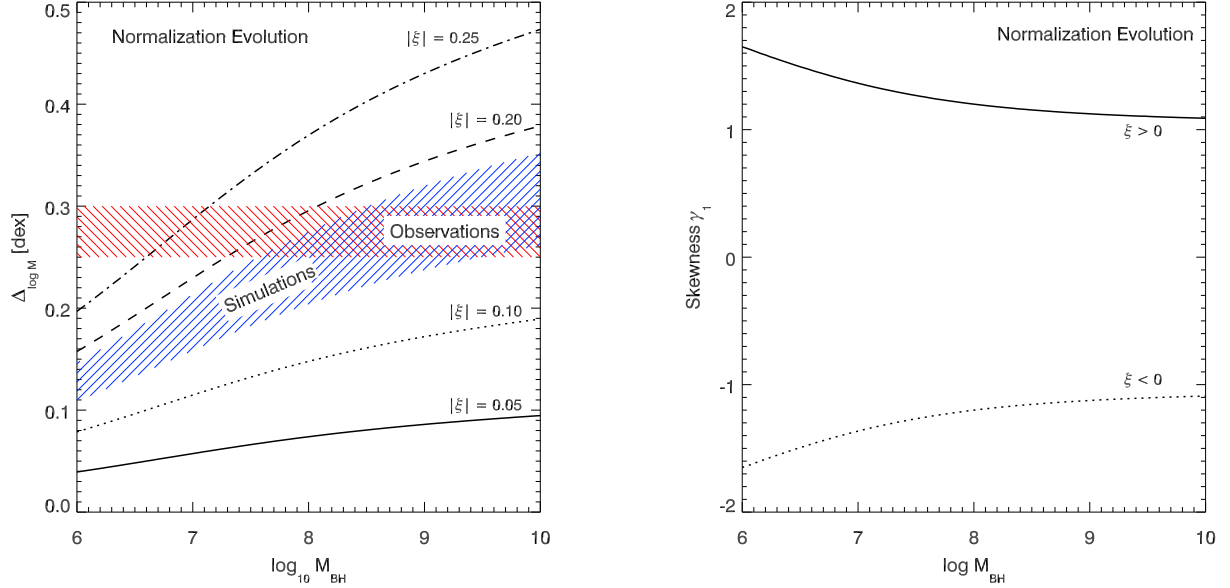


FIG. 5.— Dispersion $\Delta_{\log M_{\text{BH}}}$ and skewness γ_1 about the local $M_{\text{BH}}-\sigma$ relation caused by evolution in the normalization of the $M_{\text{BH}}-\sigma$ relation with redshift of the form $\log(M_{\text{BH}}) = \alpha + \beta \log(\sigma/\sigma_0) - \xi \log(1+z)$. The dispersion is plotted for $|\xi| = 0.05$ (solid), 0.10 (dotted), 0.20 (dashed), and 0.25 (dash-dotted). The observed dispersion $\Delta_{\log M_{\text{BH}}}^{\text{obs}} = 0.25 - 0.3$ (shaded region) constrains evolution in the normalization to approximately $|\xi| < 0.2$. If the normalization evolves, the sign of the skewness in the distribution about the local $M_{\text{BH}}-\sigma$ relation indicates the sign of ξ .

differing mass bins the result could be associated with an evolution in the $M_{\text{BH}}-\sigma$ relation. Below, we characterize the mass dependence of the statistical moments of the distribution of galaxies around the mean $M_{\text{BH}}-\sigma$ relation and relate them to possible forms for $M_{\text{BH}}-\sigma$ evolution.

4.1.1. Normalization Evolution

For a normalization evolution of the form of Equation (5), the dispersion $\Delta_{\log M_{\text{BH}}}$ and skewness γ_1 for the $M_{\text{BH}}-\sigma$ relation at $z=0$ can be readily calculated using Equations (7–8) given a $P(z_f|\log M_{\text{BH}})$ describing the evolution of the cosmic black hole population. Figure 5 shows the dispersion in black hole mass $\Delta_{\log M_{\text{BH}}}$ as a function of SMBH mass introduced in the $M_{\text{BH}}-\sigma$ relation at $z=0$ by normalization evolution over a range in the power law index ξ (left panel). As $\Delta_{\log M_{\text{BH}}}$ is an even function of ξ , we plot $\Delta_{\log M_{\text{BH}}}$ for different values of $|\xi|$. The observed range of $\Delta_{\log M_{\text{BH}}}^{\text{obs}} = 0.25 - 0.3$ dex (red shaded region) can be compared to the normalization evolution measured in the simulations of $\xi \approx 0.138 - 0.186$ (blue shaded region), and the simulations agree well with the observational constraints. Given the observational data and our chosen $P(z_f|\log M_{\text{BH}})$, evolution in the normalization with approximately $|\xi| < 0.2$ is allowed. The mass-dependence of $\Delta_{\log M_{\text{BH}}}$ directly reflects changes in the black hole population during the evolution of the $M_{\text{BH}}-\sigma$ normalization with redshift, with more massive black holes being formed during characteristically earlier epochs when the $M_{\text{BH}}-\sigma$ normalization was more discrepant from the $z=0$ relation than during the formation epoch of smaller mass black holes. As the most massive black holes form over a wider range in redshift than smaller black holes, their broader PDFs also contribute to the scatter about the mean relation. If further sources of scatter in the $M_{\text{BH}}-\sigma$ relation are unimportant and subsequent galactic evolution does not strongly effect $P(z_f|\log M_{\text{BH}})$, then the slope of $\Delta_{\log M_{\text{BH}}}$ provides direct

information about the typical redshift of formation for black holes of a given mass. We note that since the black hole and spheroids form contemporaneously in our model, the evolution owing to ξ in the calculations also suggests a correlation between the deviation of a galaxy from the $M_{\text{BH}}-\sigma$ relation and the age of the spheroidal stellar population. For normalization evolution such a correlation results from the monotonic mapping of the measured velocity dispersion deviation $\delta_{\log \sigma} \equiv [\log(\sigma(M_{\text{BH}}, z_f) - \log \sigma(M_{\text{BH}}, z=0))] = \xi \log(1+z_f)$ to a formation redshift z_f , which means the probability distribution function $P(\delta_{\log \sigma}|\log M_{\text{BH}})$ maps monotonically onto $P(z_f|\log M_{\text{BH}})$.

Further information on ξ can be gleaned from the skewness γ_1 of the distribution (Figure 5, right panel). For normalization evolution of the form of Equation (5), the resulting skewness has the same sign as the power law index and immediately indicates whether the $M_{\text{BH}}-\sigma$ normalization increases or decreases with redshift. All positive values of ξ have the same skewness, with the same functional shape as the skewness defined by negative values of ξ reflected about the origin.

4.1.2. Slope Evolution

While our simulated $M_{\text{BH}}-\sigma$ relations do not show any monotonic trend in their slope with redshift, many theories for the $M_{\text{BH}}-\sigma$ relation have some functional dependence in the slope with redshift or black hole mass (e.g. Sazonov et al. 2005; Wyithe 2005). The dispersion $\Delta_{\log M_{\text{BH}}}$ and skewness γ_1 for the $M_{\text{BH}}-\sigma$ relation owing to slope evolution of the form of Equation (9) is also accessible using the method described for characterizing normalization evolution. Figure 6 shows the dispersion $\Delta_{\log M_{\text{BH}}}$ (left panel) about the local $M_{\text{BH}}-\sigma$ relation induced by slope evolution, plotted for $\phi = 0.2$ (solid), 0.3 (dashed), -0.2 (dotted), and -0.3 (dash-dotted). To illustrate the mass dependence of $\Delta_{\log M_{\text{BH}}}$ and γ_1 above and below the pivot we choose the fixed intercept to be

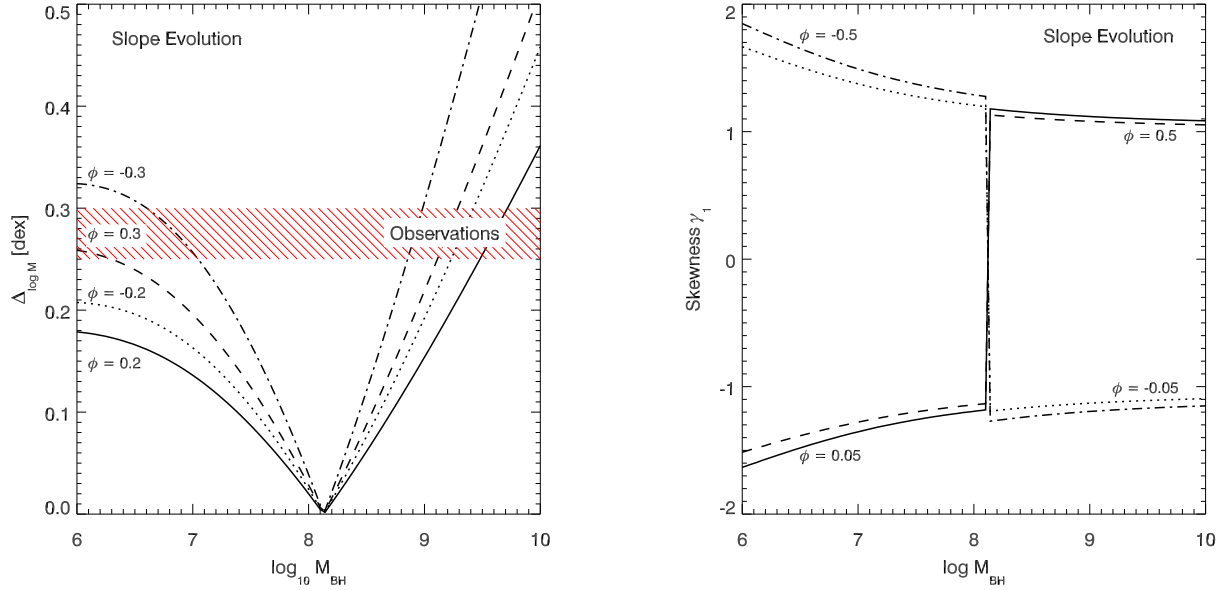


FIG. 6.— Dispersion $\Delta_{\log M_{\text{BH}}}$ (left panel) and skewness γ_1 (right panel) about the local $M_{\text{BH}}-\sigma$ relation induced by an evolution in the slope of the $M_{\text{BH}}-\sigma$ relation with redshift of the form $\log(M_{\text{BH}}) = \alpha + \beta(1+z)^\phi \log(\sigma/\sigma_0)$. The dispersion is plotted for $\phi = 0.2$ (solid), 0.3 (dashed), -0.2 (dotted), and -0.3 (dash-dotted). To illustrate the mass dependence of $\Delta_{\log M_{\text{BH}}}$ and γ_1 above and below the pivot, we choose the fixed intercept to be $\log M_{\text{BH},\text{fixed}} = \alpha = 8.13$. The observed dispersion $\Delta_{\log M_{\text{BH}}}^{\text{obs}} = 0.25 - 0.3$ (shaded region) constrains evolution in the slope to approximately $|\phi| < 0.3$. If the slope of the $M_{\text{BH}}-\sigma$ relation evolves and the intercept falls in the observable range, the sign of ϕ could be constrained by examining the sign of the observed skewness as a function of black hole mass because γ_1 changes sign at the pivot mass.

$\log M_{\text{BH},\text{fixed}} = \alpha = 8.13$, but the same analysis could be performed for any intercept. For consistency with the observed dispersion $\Delta_{\log M_{\text{BH}}}^{\text{obs}} = 0.25 - 0.3$ (shaded region), the evolution in the slope is constrained to approximately $|\phi| < 0.3$ for our chosen intercept. If the fixed pivot intercept for a slope evolution of the $M_{\text{BH}}-\sigma$ relation is small ($\log M_{\text{BH}} \approx 6$), then the constraint on $|\phi|$ would be much tighter as $\Delta_{\log M_{\text{BH}}}$ is a strong function of M_{BH} above the pivot mass. The skewness induced by a slope evolution (Figure 6, right panel) contains more information than for normalization evolution. The skewness provides a constraint on the pivot mass if the pivot falls in the observationally accessible range, as the sign of the skewness changes at this intercept in the redshift-dependent relation.

In principle, any model that produces a redshift evolution in the $M_{\text{BH}}-\sigma$ relation can be compared with the observations in a similar manner, and given a $P(z_f | \log M_{\text{BH}})$ for the cosmic black hole population, distinct models for generating the $M_{\text{BH}}-\sigma$ relation could be observationally differentiated. We note here that comparisons with observations are most meaningful if the black holes in the measured $M_{\text{BH}}-\sigma$ relation represent a fair sample of the total black hole population for a given mass bin. For instance, an increase in the number of bulges in spiral systems with well-determined M_{BH} and σ would be helpful. Unfortunately, dust effects make stellar dynamical measurements late-type galaxies difficult and a more effective approach for determining black hole masses in these systems will need further development (e.g. Ho et al. 2002). We encourage further observational efforts to eliminate selection biases in the sample used to determine the local $M_{\text{BH}}-\sigma$ relation.

4.2. Observations of $M_{\text{BH}}-\sigma$ in AGN at $z > 0$

Our simulations can be directly related to the $M_{\text{BH}}-\sigma$ relation in normal galaxies at redshifts $z > 0$. However, previous observational efforts to measure the $M_{\text{BH}}-\sigma$ relation in galaxies beyond the locally accessible sample have concentrated mostly on using the $M_{\text{BH}}-\sigma$ relation indicators in active galactic nuclei (Shields et al. 2003; Treu et al. 2004), combining $\text{H}\beta$ linewidth estimates for black hole mass (e.g. Wandel et al. 1999) and [OIII] linewidths as a proxy for stellar velocity dispersion (e.g. Nelson 2000a) or dispersion measurements from stellar spectral features (Treu et al. 2001). Other estimates for the $M_{\text{BH}}-\sigma$ relation in high- z quasars have been made (e.g. Walter et al. 2004) by comparing a black hole mass inferred from Eddington-limited accretion onto a bright quasar with the dynamical mass estimated from Very Large Array observations of molecular gas kinematics.

Shields et al. (2003) found that AGN between $z = 0 - 3.5$ obey an $\text{H}\beta$ -[OIII] relation consistent with the local $M_{\text{BH}}-\sigma$ relation determined by T02, and the observations at any single redshift were also consistent with the $z = 0$ result, though the statistics are somewhat limited. The observations of Treu et al. (2004) imply a conflicting result with seven AGN at $z \sim 0.37$ inferred to primarily lie above the $z = 0$ $M_{\text{BH}}-\sigma$ relation, though with significant scatter and large estimated error. The Walter et al. (2004) CO(3-2) observations also place the $z = 6.42$ quasar above the $z = 0$ $M_{\text{BH}}-\sigma$ relation and claim to be inconsistent with the presence of a stellar bulge of the size needed to match the local $M_{\text{BH}}-M_{\text{bulge}}$ relations.

The increased scatter observed in the AGN samples and the deviation of high- z quasars relative to our calculations may originate in the dynamical state of the observed systems (for a related discussion, see Vestergaard 2004). If these systems correspond to merging galaxies, they may not be dynamically relaxed and these samples may therefore display a larger

range of velocity dispersions than do the dynamically relaxed systems that primarily comprise the locally observed $M_{\text{BH}}-\sigma$ relation or the redshift-dependent $M_{\text{BH}}-\sigma$ relation in relaxed galaxies produced by our simulations. For instance, observations of local Seyfert galaxies show that tidally-distorted hosts have systematically higher emission line widths at a given stellar velocity dispersion (Nelson & Whittle 1996). An exploration of the $M_{\text{BH}}-\sigma$ relation during the peak AGN phases of our simulations is planned in future work, but given the current observational and theoretical uncertainties we do not believe our simulations are in conflict with the observations. However, our simulations are more consistent with the Shields et al. (2003) claim of no evolution than with either the Treu et al. (2004) or Walter et al. (2004) claims of evidence for evolution in the $M_{\text{BH}}-\sigma$ relation. In our model where the $M_{\text{BH}}-\sigma$ scaling is set during spheroid formation, the evolution of systems tends to occur either quickly in the M_{BH} direction during the exponential growth phase of the black hole or more gradually along the $M_{\text{BH}}-\sigma$ relation during self-regulated black hole growth. The presence of massive black holes at high redshift without massive bulges would be rare in the context of our modeling, and such outliers would likely have to undergo purely stellar major mergers to reach the local $M_{\text{BH}}-\sigma$ relation. We also note that if the Treu et al. (2004) offset of $\delta \log \sigma = -0.16$ measured for AGN at $z = 0.37$ holds for the $M_{\text{BH}}-\sigma$ relation generated by the merging of normal galaxies at that redshift, then a power-law evolution in the normalization of σ would imply $\xi = -1.17$. If some subsequent process does not reduce the deviation from the $z = 0$ $M_{\text{BH}}-\sigma$ relation for a given galaxy, then with our $P(z_f | \log M_{\text{BH}})$ and the evolution $\xi = -1.17$ inferred from the Treu et al. (2004) measurements, the scatter in the $M_{\text{BH}}-\sigma$ relation at $z = 0$ would be $\Delta_{\log M_{\text{BH}}} = 0.92 - 2.215$ over the range $\log M_{\text{BH}} = 6 - 10$. This scatter is much larger than both the observed dispersion and the dispersion predicted by our simulations and formation redshift distribution $P(z_f | \log M_{\text{BH}})$.

4.3. Observations of Inactive Galaxies at $z > 0$

For the next-generation of large telescopes, a measurement of the central stellar velocity dispersion in normal galaxies at high redshifts may be feasible, and our simulations can connect directly with such observations. A proper census of the cosmic black hole population as a function of redshift will necessarily involve an estimate of the mass of SMBHs at the centers of inactive galaxies. Without black hole activity to provide an estimate of the black hole mass, and given the likely prohibitively extreme resolution (< 10 pc) needed for stellar dynamical estimates of SMBH masses, inferring black hole masses through the $M_{\text{BH}}-\sigma$ relation via stellar velocity dispersion measures for the cosmological spheroid population may provide the best way of constraining the evolution of the black hole population with redshift. These measurements will necessarily involve an assumed model to relate M_{BH} and σ as a function of redshift, such as the relation calculated by our simulations. Our work then provides additional theoretical motivation for attempting these observations with future generations of large infrared-capable telescopes.

Among the large telescopes currently in various stages of development are the Giant Magellan Telescope (GMT, Johns et al. 2004, 20-25m), California Extremely Large Telescope (CELT, Nelson 2000b, 30m), Euro50 (Andersen et al. 2004, 50m), OverWhelmingly Large Telescope (OWL, Dierickx et al. 2004, 100m), Japanese Extremely Large Telescope (Iye et al. 2004, 30m), and the Chinese Future Giant

Telescope (Ding-Qiang et al. 2004, 30m). The planned capabilities of these telescopes are impressive. For instance, the GMT design calls for a resolution of $\theta_{\text{GLAO}} \approx 0.15''$ with ground layer adaptive optics (GLAO) and $\theta_{\text{FAO}} \approx 0.007''$ with fully adaptive optics (FAO), corresponding to physical scales at redshift $z = 3$ of $R_{\text{GLAO}} \approx 1.15$ kpc and $R_{\text{FAO}} \approx 54$ pc, respectively. The remnant systems in our simulations appropriate for $z = 3$ progenitors have effective radii ranging from $R_{\text{eff}} \approx 0.3 - 10$ physical kpc, making central stellar velocity dispersion measurements feasible in principle, and likely possible even with GLAO observations for the most massive systems. Infrared spectroscopy of rest-frame UV stellar lines could be used to find central stellar velocity dispersions of spheroids and, combined with the simulation results to estimate M_{BH} via an inversion of the calculated $M_{\text{BH}}-\sigma$ relation for a given redshift, the cosmic black hole population can be constrained (see, e.g. Yu & Tremaine 2002). In addition, if SMBH feedback is important to determining the properties of normal galaxies (e.g. Springel et al. 2004; Robertson et al. 2005), such observations could prove to be crucial input for theories of galaxy formation during the evolutionary epoch when the most massive black holes are formed.

5. DISCUSSION

Our simulations demonstrate that the merging of disk galaxies whose properties are appropriate for redshifts $z = 0 - 6$ should produce an $M_{\text{BH}}-\sigma$ relation with the observed power-law scaling $M_{\text{BH}} \propto \sigma^4$. The $M_{\text{BH}}-\sigma$ relation retains this scaling at redshifts $z = 0 - 6$, even while the merger progenitors range widely in their structural properties with redshift. A possible weak evolution in the normalization of the $M_{\text{BH}}-\sigma$ relation is found, which may result from an increasing velocity dispersion owing to the redshift evolution of the potential wells of galaxies. Simple arguments for how such evolution would affect the velocity dispersion provide a similar redshift scaling at redshifts $z = 2 - 6$ to those calculated from the simulations. As these redshift scalings systematically place high-redshift systems below the $z = 0$ $M_{\text{BH}}-\sigma$ relation, subsequent accretion processes may further reduce the scatter in the observed $M_{\text{BH}}-\sigma$ relation over time.

Our results also provide guidance to semi-analytical models about the behavior of the $M_{\text{BH}}-\sigma$ relation. We suggest that semi-analytical models in the vein of Volonteri et al. (2003) or Menci et al. (2003) could be altered to explicitly maintain the local $M_{\text{BH}}-M_{\text{bulge}}$ relation at redshifts $z < 6$, produce the same $M_{\text{BH}}-\sigma$ scaling at redshifts $z < 6$, and reproduce the local $M_{\text{BH}}-\sigma$ normalization. Simultaneously such models should tie morphological information, such as spheroid growth, to the growth of supermassive black holes (for a related discussion, see Bromley et al. 2004). While some semi-analytical models include prescriptions for black hole accretion or feedback (e.g. Menci et al. 2003; Wyithe & Loeb 2003), it is difficult to graft all the effects of feedback onto these models without a detailed treatment of the complex interplay between gas inflows, starbursts, and black hole activity. These models could also be altered to more fully capture the black hole mass-dependent effects of feedback on galaxies and their environments (see also, e.g., Hopkins et al. 2005e).

Overall, our simulations provide more general conclusions about the cosmological evolution of structure. The spheroidal components of galaxies are likely formed in the same process that sets the $M_{\text{BH}}-\sigma$ relation and therefore the demographics of black holes traces the demographics of spheroids over cosmic time, as is inferred locally (Yu & Tremaine 2002).

With the possible shared origin of spheroids and SMBHs in mind, we note that observations suggest the stellar populations of cluster ellipticals form at redshifts $z > 2$ (e.g. van Dokkum & Stanford 2003; Gebhardt et al. 2003). This era coincides with the epoch $z \sim 3$ during which the most massive SMBHs are formed, as inferred from the evolution in the quasar number density (Schmidt et al. 1995; Boyle et al. 2000). Future comparisons with high-redshift AGN and massive ellipticals could help provide our modeling of individual mergers with a broader cosmological context. By connecting with the evolution of the observed quasar luminosity function through the $P(z_f | \log M_{\text{BH}})$ supplied by calculations in the vein of Hopkins et al. (2005e), our model may account for cosmological considerations such as evolution in either the mass-dependent galaxy merger rate, the cold gas fraction, or the global star formation rate.

While uncertainties remain in our method, an analysis similar to that presented here could be performed for simulations with different treatments of the relevant physics of black hole accretion and feedback, star formation, or ISM processes. As the observational data improve, the comparisons presented in this paper could be used to constrain the physical prescriptions used in simulations of galaxy formation. For instance, our knowledge of possible redshift-dependence in the thermal coupling η_{therm} of black hole feedback to the gas is limited. The normalization of the $M_{\text{BH}}-\sigma$ relation depends on η_{therm} for a given accretion model, and a strong increase in η_{therm} would introduce a correspondingly larger scatter in the $M_{\text{BH}}-\sigma$ relation at $z = 0$. A decrease in the thermal coupling with redshift would decrease the scatter at $z = 0$, but in principle this effect could be counteracted if the dominant mode of black hole accretion is more efficient at higher redshifts. Better observational samples will help inform our modeling of these physics by improving constraints from the statistical moments of the $z = 0 M_{\text{BH}}-\sigma$ relation.

While our method for comparing evolution in the $M_{\text{BH}}-\sigma$ relation with observational constraints involves adopting a probability distribution function $P(z_f | \log M_{\text{BH}})$ relating black hole mass with a characteristic formation redshift, the general formalism does not depend on the particular choice of $P(z_f | \log M_{\text{BH}})$ or the corresponding interpretation of the quasar luminosity function. A similar analysis may be repeated for other theoretical frameworks connecting galaxy formation to supermassive black hole growth.

Lastly, the robust nature of the $M_{\text{BH}}-\sigma$ relation produced by our simulations suggests that the merging of galaxies over cosmic time will produce a relation with small intrinsic scatter, in accord with observations. The weak evolution of the calculated $M_{\text{BH}}-\sigma$ normalization implies that the small observed scatter in the $M_{\text{BH}}-\sigma$ reflects the robust physical origin of the relation (e.g. Haehnelt & Kauffmann 2000). While the dispersion $\Delta_{M_{\text{BH}}} = 0.25 - 0.3$ measured by Tremaine et al. (2002) is estimated to be intrinsic to the $M_{\text{BH}}-\sigma$ relation, if the observational errors have been significantly underestimated then our physical model may need improvement. We note that preliminary evidence of a second parameter in the $M_{\text{BH}}-\sigma$ relation (Siopis et al. 2004) may be connected to statistical variance introduced by a redshift-dependent normalization, which may take the form of either a correlation with galaxy morphology or environment. Further comparisons between the observational data and simulations could help clarify these possibilities, especially in a cosmological setting. The redshift evolution of the Faber-Jackson relation measured in the remnants may bear on observations of the fundamental plane

(Dressler et al. 1987; Djorgovski & Davis 1987) and will be explored in forthcoming work.

6. SUMMARY

We calculate the $M_{\text{BH}}-\sigma$ relation produced by the merging of disk galaxies appropriate for redshifts $z = 0, 2, 3$, and 6 using a large set of 112 hydrodynamic simulations that include the effects of feedback from accreting supermassive black holes and supernovae. We develop a method for comparing the $M_{\text{BH}}-\sigma$ relation produced by simulations with existing observational constraints through the statistical moments of the measured relation using the formalism presented by Yu & Lu (2004), and find the simulations to be in agreement with the dispersion $\Delta_{\log M_{\text{BH}}} = 0.25 - 0.3$ reported by Tremaine et al. (2002). The conclusions of our work are:

- The simulations suggest that the normalization of the $M_{\text{BH}}-\sigma$ relation may experience a weak evolution with redshift while the slope is consistent with being constant near the locally observed value of $\beta \sim 4$ (Ferrarese & Merritt 2000; Gebhardt et al. 2000). As our simulations cover a wide range of virial mass, gas fraction, ISM pressurization, dark matter halo concentration, and surface mass density at each redshift, our results suggest the physics that set the $M_{\text{BH}}-\sigma$ scaling are remarkably insensitive to the properties of progenitor galaxies in the scenario where the $M_{\text{BH}}-\sigma$ relation is created through coupled black hole and spheroid growth in galaxy mergers.
- We demonstrate how to compare theoretical models for the $M_{\text{BH}}-\sigma$ relation that predict redshift evolution in either the slope or normalization to the observed $M_{\text{BH}}-\sigma$ relation by calculating the $z = 0$ dispersion $\Delta_{\log M_{\text{BH}}}$ of the relation given a functional form for the evolution and a probability distribution function $P(z_f | \log M_{\text{BH}})$ that relates black hole mass to a characteristic formation redshift. Adopting a model for $P(z_f | \log M_{\text{BH}})$ from Hopkins et al. (2005e), we calculate the allowed strength of redshift evolution given power-law, redshift evolution in either normalization or slope consistent with the observed scatter at $z = 0$. The modest normalization evolution calculated by our simulations produces a scatter similar to that observed. We demonstrate how redshift evolution in the $M_{\text{BH}}-\sigma$ relation introduces mass-dependent dispersion and skewness about the average relation, and show how these statistical moments can be used to differentiate theoretical models for the $M_{\text{BH}}-\sigma$ relation that predict distinct redshift evolutions.
- We relate our simulations to observations of the $M_{\text{BH}}-\sigma$ relation in AGN at redshifts $z > 0$ and, given the observational and theoretical uncertainties, find the properties of our inactive remnants to be more consistent with the redshift-independent $M_{\text{BH}}-\sigma$ relation measured by Shields et al. (2003) than the claims of Treu et al. (2004) and Walter et al. (2004) that supermassive black holes may form earlier than galactic spheroids. We show that if the offset $\delta \log \sigma = -0.16$ in the $M_{\text{BH}}-\sigma$ relation measured by Treu et al. (2004) for AGN at $z = 0.37$ is attributed to a power-law evolution in the normalization of the velocity dispersion as $\sigma(z) \propto \sigma(z=0)(1+z)^\xi$, the resultant scatter expected in the $z = 0 M_{\text{BH}}-\sigma$ relation would be much larger than is

observed. Additional comparisons between the active phase of our merger simulations and the observations of active galaxies are planned in future work.

- Our simulations provide additional motivation for future observations of high-redshift normal galaxies using the next-generation of large telescopes for the purpose of constraining the evolution of the cosmic black hole population with time. The planned 20–30m-class telescopes with infrared spectrographs should be able to measure central stellar velocity dispersions in galaxies to $z \sim 3$. Our simulations can be used to connect those measurements to estimates for the supermassive black hole mass function and the distribution of black hole formation redshifts $P(z_f | \log M_{\text{BH}})$. A complete census of the cosmic black hole population will require measurements of the spheroid population at high redshifts and will serve as important input into structure formation theories that account for the effects of black hole feedback on normal galaxies.

REFERENCES

Adams, F. C., Graff, D. S., Mbonye, M., & Richstone, D. O. 2003, ApJ, 591, 125

Adams, F. C., Graff, D. S., & Richstone, D. O. 2001, ApJ, 551, L31

Andersen, T. E., et al. 2004, in Proceedings of the SPIE, 5489, 407

Archibald, E. N., Dunlop, J. S., Jimenez, R., Friaça, A. C. S., McLure, R. J., & Hughes, D. H. 2002, MNRAS, 336, 353

Baes, M., Buyle, P., Hau, G. K. T., & Dejonghe, H. 2003, MNRAS, 341, L44

Balberg, S., & Shapiro, S. L. 2002, Physical Review Letters, 88, 101301

Bernardi, M., et al. 2003, AJ, 125, 1866

Bondi, H. 1952, MNRAS, 112, 195

Bondi, H., & Hoyle, F. 1944, MNRAS, 104, 273

Boyle, B. J., Shanks, T., Croom, S. M., Smith, R. J., Miller, L., Loaring, N., & Heymans, C. 2000, MNRAS, 317, 1014

Bromley, J. M., Somerville, R. S., & Fabian, A. C. 2004, MNRAS, 350, 456

Bullock, J. S., Kolatt, T. S., Sigad, Y., Somerville, R. S., Kravtsov, A. V., Klypin, A. A., Primack, J. R., & Dekel, A. 2001, MNRAS, 321, 559

Burkert, A., & Silk, J. 2001, ApJ, 554, L151

Ciotti, L., & van Albada, T. S. 2001, ApJ, 552, L13

Cowie, L. L., Barger, A. J., Bautz, M. W., Brandt, W. N., & Garmire, G. P. 2003, ApJ, 584, L57

Cox, T. J., Di Matteo, T., Hernquist, L., Hopkins, P. F., Robertson, B., & Springel, S. 2005, ApJ, submitted, astro-ph/0504156

Di Matteo, T., Croft, R. A. C., Springel, V., & Hernquist, L. 2003, ApJ, 593, 56

—. 2004, ApJ, 610, 80

Di Matteo, T., Springel, V., & Hernquist, L. 2005, Nature, 433, 604

Dierickx, P., et al. 2004, in Proceedings of the SPIE, 5489, 391

Ding-Qiang, S., Ya-nan, W., & Xiangqun, C. 2004, in Proceedings of the SPIE, 5489, 429

Djorgovski, S., & Davis, M. 1987, ApJ, 313, 59

Dressler, A., Lynden-Bell, D., Burstein, D., Davies, R. L., Faber, S. M., Terlevich, R., & Wegner, G. 1987, ApJ, 313, 42

Eckart, A., & Genzel, R. 1997, MNRAS, 284, 576

Faber, S. M., & Jackson, R. E. 1976, ApJ, 204, 668

Faber, S. M., et al. 1997, AJ, 114, 1771

Fabian, A. C. 1999, MNRAS, 308, L39

Ferrarese, L. 2002, ApJ, 578, 90

Ferrarese, L., & Merritt, D. 2000, ApJ, 539, L9

Gebhardt, K., et al. 2000, ApJ, 539, L13

Gebhardt, K., et al. 2003, ApJ, 597, 239

Gezhe, A. M., Klein, B. L., Morris, M., & Becklin, E. E. 1998, ApJ, 509, 678

Gingold, R. A., & Monaghan, J. J. 1977, MNRAS, 181, 375

Granato, G. L., Silva, L., Monaco, P., Panuzzo, P., Salucci, P., De Zotti, G., & Danese, L. 2001, MNRAS, 324, 757

Haehnelt, M. G., & Kauffmann, G. 2000, MNRAS, 318, L35

Haiman, Z., & Loeb, A. 1998, ApJ, 503, 505

Hernquist, L. 1990, ApJ, 356, 359

Ho, L. C., Sarzi, M., Rix, H., Shields, J. C., Rudnick, G., Filippenko, A. V., & Barth, A. J. 2002, PASP, 114, 137

Hopkins, P. F., Hernquist, L., Martini, P., Cox, T. J., Robertson, B., Di Matteo, T., & Springel, S. 2005a, ApJ, accepted, astro-ph/0502241

Hopkins, P. F., Hernquist, L., Cox, T. J., Di Matteo, T., Martini, P., Robertson, B., & Springel, S. 2005b, ApJ, accepted, astro-ph/0504190

—. 2005c, ApJ, accepted, astro-ph/0504252

—. 2005d, ApJ, submitted, astro-ph/0504253

Hopkins, P. F., Hernquist, L., Cox, T. J., Di Matteo, T., Robertson, B., & Springel, S. 2005e, ApJ, in preparation

Hoyle, F., & Lyttleton, R. A. 1939, in Proceedings of the Cambridge Philosophical Society, 405–

Iye, M., et al. 2004, in Proceedings of the SPIE, 5489, 417

Johns, M., Angel, J. R. P., Shectman, S., Bernstein, R., Fabricant, D. G., McCarthy, P., & Phillips, M. 2004, in Proceedings of the SPIE, Volume 5489, pp. 441–453 (2004), 441–453

Kauffmann, G., & Haehnelt, M. 2000, MNRAS, 311, 576

Kazantzidis, S., et al. 2005, ApJ, 623, L67

King, A. 2003, ApJ, 596, L27

Kormendy, J., & Richstone, D. 1995, ARA&A, 33, 581

Lucy, L. B. 1977, AJ, 82, 1013

MacMillan, J. D., & Henriksen, R. N. 2002, ApJ, 569, 83

Magorrian, J., et al. 1998, AJ, 115, 2285

Marconi, A., & Hunt, L. K. 2003, ApJ, 589, L21

McKee, C. F., & Ostriker, J. P. 1977, ApJ, 218, 148

Menci, N., Cavaliere, A., Fontana, A., Giallongo, E., Poli, F., & Vittorini, V. 2003, ApJ, 587, L63

Menou, K., Haiman, Z., & Narayan, V. K. 2001, ApJ, 558, 535

Miralda-Escudé, J., & Kollmeier, J. A. 2005, ApJ, 619, 30

Miyoshi, M., Moran, J., Hernstein, J., Greenhill, L., Nakai, N., Diamond, P., & Inoue, M. 1995, Nature, 373, 127

Mo, H. J., Mao, S., & White, S. D. M. 1998, MNRAS, 295, 319

Monaco, P., Salucci, P., & Danese, L. 2000, MNRAS, 311, 279

Murray, N., Quataert, E., & Thompson, T. A. 2005, ApJ, 618, 569

Navarro, J. F., Frenk, C. S., & White, S. D. M. 1997, ApJ, 490, 493

Nelson, C. H. 2000a, ApJ, 544, L91

Nelson, C. H., & Whittle, M. 1996, ApJ, 465, 96

Nelson, J. E. 2000b, in Proc. SPIE Vol. 4004, p. 282–289, Telescope Structures, Enclosures, Controls, Assembly/Integration/Validation, and Commissioning, Thomas A. Sebring; Torben Andersen; Eds., 282–289

Nipoti, C., Londrillo, P., & Ciotti, L. 2003, MNRAS, 342, 501

Richstone, D., et al. 1998, Nature, 395, A14+

Robertson, B., Hernquist, L., Bullock, J. S., Cox, T. J., Di Matteo, T., Springel, V., & Yoshida, N. 2005, ApJ, submitted, astro-ph/0503369

Robertson, B., Yoshida, N., Springel, V., & Hernquist, L. 2004, ApJ, 606, 32

Sazonov, S. Y., Ostriker, J. P., Ciotti, L., & Sunyaev, R. A. 2005, MNRAS, 128

Schmidt, M., Schneider, D. P., & Gunn, J. E. 1995, AJ, 110, 68

Shields, G. A., Gebhardt, K., Salvander, S., Wills, B. J., Xie, B., Brotherton, M. S., Yuan, J., & Dietrich, M. 2003, ApJ, 583, 124

Siegel, M. H., Majewski, S. R., Reid, I. N., & Thompson, I. B. 2002, ApJ, 578, 151

Silk, J., & Rees, M. J. 1998, A&A, 331, L1

Siopis, C., et al. 2004, American Astronomical Society Meeting Abstracts, 205

Springel, V. 2005, MNRAS, Submitted.

Springel, V., Di Matteo, T., & Hernquist, L. 2004, MNRAS, Submitted.

Springel, V., Di Matteo, T., & Hernquist, L. 2005, ApJ, 620, L79

Springel, V., & Hernquist, L. 2002, MNRAS, 333, 649

—. 2003, MNRAS, 339, 289

Springel, V., Yoshida, N., & White, S. D. M. 2001, New Astronomy, 6, 79

Steffen, A. T., Barger, A. J., Cowie, L. L., Mushotzky, R. F., & Yang, Y. 2003, ApJ, 596, L23

Toomre, A. 1977, in Evolution of Galaxies and Stellar Populations, 401–+

Tremaine, S., et al. 2002, ApJ, 574, 740

Treu, T., Malkan, M. A., & Blandford, R. D. 2004, ApJ, 615, L97

Treu, T., Stiavelli, M., Møller, P., Casertano, S., & Bertin, G. 2001, MNRAS, 326, 221

van Dokkum, P. G., & Stanford, S. A. 2003, ApJ, 585, 78

Vestergaard, M. 2004, ApJ, 601, 676

Vitvitska, M., Klypin, A. A., Kravtsov, A. V., Wechsler, R. H., Primack, J. R., & Bullock, J. S. 2002, ApJ, 581, 799

Volonteri, M., Haardt, F., & Madau, P. 2003, ApJ, 582, 559

Walter, F., Carilli, C., Bertoldi, F., Menten, K., Cox, P., Lo, K. Y., Fan, X., & Strauss, M. A. 2004, ApJ, 615, L17

Wandel, A. 2002, ApJ, 565, 762

Wandel, A., Peterson, B. M., & Malkan, M. A. 1999, ApJ, 526, 579

Wyithe, J. S. B., & Loeb, A. 2003, ApJ, 595, 614

Wyithe, J. S. B., 2005, MNRAS, submitted, astro-ph/0503435

Yu, Q., & Lu, Y. 2004, ApJ, 602, 603

Yu, Q., & Tremaine, S. 2002, MNRAS, 335, 965